Biochemical and Biophysical Research Communications 436 (2013) 595–600

Contents lists available at SciVerse ScienceDirect

Biochemical and Biophysical Research Communications

journal homepage: www.elsevier.com/locate/ybbrc

Mutation of cysteine residues alters the heme-binding pocket of indoleamine 2,3-dioxygenase-1

Christopher J.D. Austin [a,b], Priambudi Kosim-Satyaputra [a,1], Jason R. Smith [a], Robert D. Willows [a], Joanne F. Jamie [a,*]

[a] Department of Chemistry and Biomolecular Sciences, Macquarie University, Sydney, Australia
[b] School of Chemistry, The University of Sydney, Sydney, Australia

ARTICLE INFO

Article history:
Received 24 May 2013
Available online 7 June 2013

Keywords:
Tryptophan metabolism
Kynurenine pathway
Indoleamine 23-dioxygenase
Site-directed mutagenesis
Cysteine residues
Altered substrate binding site

ABSTRACT

The hemoprotein indoleamine 2,3-dioxygenase-1 (IDO1) is the first and rate-limiting enzyme in mammalian tryptophan metabolism. Interest in IDO1 continues to grow, due to the ever expanding influence IDO1 plays in the immune response. This study examined the contribution of all individual cysteine residues towards the overall catalytic properties and stability of recombinant human IDO1 *via* mutagenesis studies using a range of biochemical and spectroscopic techniques, including *in vitro* kinetic assessment, secondary structure identification *via* circular dichroism spectroscopy and thermal stability assessment. Upon mutation of cysteine residues we observed changes in secondary structure (principally, shifting from α-helix/β-sheet features to random coil structures) that produced out of plane heme torsion and puckering, changes to thermal stability (including gains in stability for one mutant protein) and differences in enzymatic activity (such as, increased ability to convert non-natural substrates, *e.g.*D-tryptophan) from wild type IDO1 enzyme.

1. Introduction

The haemoprotein indoleamine 2,3-dioxygenase-1 (IDO1; EC 1.13.11.52) is an immunoregulatory enzyme responsible for the oxidative cleavage of L-tryptophan to *N*′-formylkynurenine as the first step of the Kynurenine Pathway; the major metabolic pathway for tryptophan breakdown (Fig. 1; Left). Increased expression of IDO1, principally by IFN-γ release due to inflammation resulting from infection and/or disease, elicits both innate and adaptive immune responses that can have both beneficial and detrimental consequences. For example, essential amino acid removal such as tryptophan depletion by increased expression of IDO1 is an ancient, efficient and innate method of slowing the growth of infectious agents that rely on endogenous tryptophan stores for continued metabolic activity [1]. Furthermore, the low tryptophan cellular environment changes adaptive immune mechanisms, altering modulatory signals to/from T-lymphocytes, resulting in both G1-cell cycle arrest and apoptosis. This in turn causes host immunosuppression and is a major mechanism of both tumour immune escape [2] and prevention of maternal foetal rejection [3,4]. In addition, IDO1 activity affects the production of down-stream metabolites of tryptophan (e.g. 3-hydroxykynurenine and quinolinic acid), which have been shown to play roles in inflammatory disease symptomology, particularly in the CNS [5,6]. Consequently, IDO1 has received significant research attention as a potential therapeutic target in disease states where the immune system is in a state of dysregulation, for example, ovarian cancer [7]. A greater understanding of how the structural components of human IDO1 interact (*vide infra*), and how alteration of these interactions govern both function and stability, may aid both future drug development and identification and characterisation of possible deleterious single nucleotide polymorphisms [8].

Cysteine residues in proteins are important sites for metal coordination, catalysis and structure stabilisation. Containing a reactive sulfhydryl (–SH) group, the cysteine moiety can act as a nucleophile and forms thiol radicals, making it possible to form both intra- and intermolecular covalent bonds. However, the ease of formation of such covalent bonds depends on the overall redox potential, the spatial environment and pH of the protein and surrounding environment. In IDO1, cysteines are well distributed, mostly in helices. Three cysteine residues are found in the small domain (which contains nine α-helices and two β-sheets) and five in the large domain (comprising 15 α-helices and the catalytic pocket – Fig. 1; Right). IDO1 cysteines do not form disulfide bridges or co-ordinate to the heme iron so their role in the maintenance of activity/structure remains largely unknown. We report here on the contribution of all the individual cysteine residues towards the

* Corresponding author. Address: Department of Chemistry and Biomolecular Sciences, Macquarie University, NSW 2109, Australia. Fax: +61 2 9850 8313.
E-mail address: joanne.jamie@mq.edu.au (J.F. Jamie).

[1] We are particularly grateful for Dr Kosim-Satyaputra's contribution to this research. Sadly, Priambudi passed away before this manuscript could be submitted for publication.

0006-291X/$ - see front matter © 2013 Elsevier Inc. All rights reserved.
http://dx.doi.org/10.1016/j.bbrc.2013.05.119

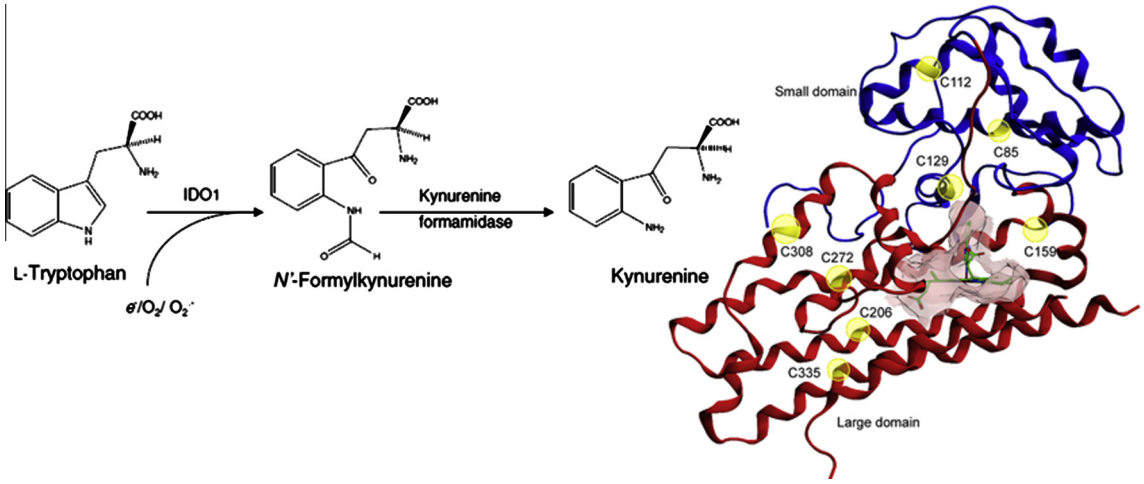

Fig. 1. (Left): initial steps of the Kynurenine pathway. The heme containing enzyme indoleamine 2,3-dioxygenase (IDO) is capable of catalysing this reaction. The cleavage product, *N*′-formylkynurenine, is then hydrolysed by kynurenine formamidase, or spontaneously, to form kynurenine. (Right) Crystal structure of human IDO-1 showing positions of all 8 cysteine residues and the active site (PDB: 2D0T, [16]). Active site – pink; heme and co-crystalised phenylimidazole – green. The large and small domains are coloured red and blue, respectively. (For interpretation of the references to colour in this figure legend, the reader is referred to the web version of this article.)

overall catalytic properties, secondary structure, heme environment and stability of human IDO1.

2. Materials and methods

2.1. Materials

All chemicals were of analytical grade unless otherwise specified. A Hi-Trap chelating column and Microspin Sephadex G-25 columns were obtained from Amersham Biosciences. Sephadex G25 (NAP 10) columns were purchased from Pharmacia Biotech. Amicon Ultra 4 mL centrifugal devices were obtained from Millipore. A Superdex 75 PC 3.2/30 column was purchased from Pharmacia LKB Biotechnology. δ-Aminolevulinic acid (ALA), ampicillin, ascorbic acid, catalase (bovine), imidazole, isopropyl-β-D-thiogalactopyranoside (IPTG), L-kynurenine, kanamycin, lysozyme, *p*-dimethylaminobenzaldehyde (*p*-DMAB), phenylmethylsulfonylfluoride (PMSF) and L-tryptophan were obtained from Sigma–Aldrich. Bovine serum albumin (BSA) (Fraction V) was obtained from Amersham. Coomassie blue R250 was purchased from Bio-Rad. DNase and EDTA-free cocktail inhibitor tablets were products of Roche.

2.2. Site-directed mutagenesis of the IDO1 expression plasmid pQE9-IDO1

Plasmid DNA was isolated using a GenElute Plasmid Miniprep Kit (Sigma), according to the manufacturer's instructions. Site-directed mutagenesis of pQE9-IDO1 was undertaken using the QuikChange® site-directed mutagenesis kit (Stratagene) per the manufacturer's instructions. All primers were synthesised by Sigma–Genosys (Castle Hill, Australia). Primers used for site-directed mutagenesis and sequencing are outlined in Supplementary Data. Dye terminator DNA sequence analysis was performed using an ABI-PRISM 377 DNA sequencer (Applied Biosystems) to confirm mutations.

2.3. Bacterial Strain

The *Escherichia coli* strain (EC538, pREP4) used for expression studies has been previously used for the recombinant expression of human IDO1 [9]. Briefly, a single colony of *E. coli* (EC538) cells containing plasmids pQE9-IDO and pREP4 was inoculated in 100 mL LB medium and cultured overnight. The 100 mL culture was added to 900 mL of the same medium and incubated at 30 °C to an optical density of 0.6 at 600 nm. IPTG (100 mM), ALA (500 mM), and PMSF (1 M) were then added at final concentrations of 0.1, 0.5, and 1 mM, respectively. Each culture was incubated for a further 3 h. Cells were collected as a pellet by centrifugation at 5000*g* for 20 min at 4 °C. The pellet was suspended in 20 mL ice-cold (Dulbecco's) phosphate–buffered saline (PBS) containing 1 mM PMSF and centrifuged at 3000*g* for 15 min at 4 °C. The bacterial pellet was stored at −20 °C.

2.4. Purification of wild type IDO1 and mutant IDO1 proteins

One litre pellets of bacterial culture, obtained according to the method described above, was suspended in 25 mM tris(hydroxymethyl)methylamine (Tris) buffer at pH 7.4, containing 150 mM NaCl, 10 mM imidazole, 10 mM $MgCl_2$ and 1 mM PMSF. The suspension was then centrifuged at 5000*g* for 20 min at 4 °C and the supernatant discarded to remove any residual PBS storage buffer.

The newly washed pellets were resuspended in 20 mL of ice-cold buffer as outlined above, with the addition of EDTA free-cocktail inhibitor tablets (×2) and DNase (<1 mg). The suspension was French pressed three times at 10,000 p.s.i. and centrifuged at 5000*g* for 20 min to obtain a clear supernatant and pellet. The clear supernatant (20 mL) was then applied to a 1 mL Hi-Trap chelating column charged with nickel ions; equilibrated with the basal buffer [Tris 25 mM pH 7.4; 150 mM NaCl; 1 mM PMSF] containing 10 mM imidazole. After washing with 18 mL of this buffer, IDO1 (wild type or mutant) protein was eluted on a stepwise gradient incorporating washings at imidazole concentrations of 30, 40, 50, 65, 80 mM, and elution at 190 mM.

The protein collected at the elution step was then buffer-exchanged into 50 mM Tris pH 7.4 using a Sephadex G25 (NAP 10) column. The desalted fractions were pooled and concentrated to a volume of 50 μL using an Amicon Ultra 4 mL centrifugal device with a 30,000 Da molecular weight cut-off. The concentrated fraction was then applied to a Superdex 75 PC 3.2/30 column according to the manufacturer's instructions, after equilibration with 50 mM Tris pH 7.4. Fractions were collected in 75 μL aliquots at a flow rate of 60 μL/min over 3.5 mL. The fractions with the highest 406:280 nm absorbance were pooled for analysis.

2.5. Analysis of wild type IDO1 and mutant IDO1 proteins

Protein concentration was determined with Bio-Rad dye reagent using BSA (0–1 mg/mL) as the standard. The coloured prod-

uct was measured at 595 nm using a Shimadzu UV–Vis spectrophotometer. Proteins were visualised using SDS–PAGE analysis by the method of Laemmli [10]. Ultraviolet (UV) and visible (Vis) spectra of proteins were recorded with a Shimadzu UV–Vis spectrophotometer, with 1 cm pathlength quartz cuvettes. Circular dichroism (CD) spectra were recorded on a JASCO J-810 spectropolarimeter with 1 cm and 1 mm pathlength quartz cuvettes. Sensitivity was 100 millidegrees, and the scanning speed was 50 nm/min for an accumulation of 32 scans. Further analysis of CD data was undertaken using the CDpro and K2D programs according to established protocols [11,12]. Thermal transition curves were measured by monitoring $\lambda = 222$ nm as a function of the increasing temperature over the range 20–99 °C at 1 °C/min. T_m values were determined by finding the first derivative of the thermal transition curve using peak processing software packaged with the JASCO J-810 spectropolarimeter.

2.6. Kinetic studies

IDO1 activity was determined as described by Takikawa et al. [13] with minor modifications. In brief, the standard reaction mixture (200 μL) contained 50 mM potassium phosphate buffer (pH 6.5), 20 mM ascorbic acid (neutralised with NaOH), 200 μg/mL catalase, 10 μM methylene blue, 400 μM L-tryptophan, and IDO1 (either wild type or mutant protein). The reaction was carried out at 37 °C for 60 min and stopped by the addition of 40 μL of 30% (w/v) trichloroacetic acid. After heating at 65 °C for 15 min, the reaction mixtures were centrifuged at 11,500*g* for 7 min. The supernatant (125 μL) was transferred into a well of a 96-well microtitre plate and mixed with 125 μL of 2% (w/v) *p*-DMAB in acetic acid. The yellow pigment derived from kynurenine was measured at 480 nm using a Fluorostar microtitre plate reader (BMG Lab Technologies). A standard curve of L-kynurenine was used to determine product formation, ranging in concentration from 0–500 μM.

Using this assay, the kinetic activity of wild type IDO1 and the IDO1 mutants was determined against two substrates, *i.e.* L-tryptophan and D-tryptophan. As IDO1 enzyme samples were a mixture of active holoenzyme (heme-containing IDO1) and inactive apoenzyme (heme-free IDO1), the kinetic parameters were determined as a function of concentration of holoenzyme [14]. The concentration of holoenzyme for each sample was resolved using the extinction coefficient at 406 nm for rabbit intestinal IDO1 of $\varepsilon = 140\ mM^{-1}\ cm^{-1}$ [15]. The amount of wild type and mutant protein was adjusted to give an initial velocity for each substrate where the percentage of conversion of substrate at each concentration was less than 10%. Apparent Michaelis–Menten constants (K_m, V_{max}) were determined by varying concentrations of L-tryptophan and D-tryptophan with concentration ranges of 0–200 μM and 0–3000 μM, respectively. Each reaction was conducted in triplicate.

3. Results and discussion

3.1. Structural analysis of wild type and mutant IDO1 species

Following the purification of the wild type and mutant IDO1 proteins, the products obtained were subjected to SDS–PAGE analysis. For each isolated protein, one homologous band was observed with a molecular mass of ~45 kDa (data not shown).

Far UV CD spectra were obtained and analysed using Cdpro and K2D3 deconvolution programs to determine whether Cysteine (C) to Alanine (A) mutations changed the secondary structure of IDO1 when compared to wild type (Fig. 2A). The analyses showed that wild type IDO1 protein exhibited a configuration consisting of 63% α-helical, 4% β-sheet and 33% random coil (Table 1); consistent with the known secondary structure of human IDO1 elucidated from Sugimoto et al.'s crystal structure [16]. The mutant IDO1 proteins differed in structural composition when compared to wild type enzyme (Table 1- 38–71% α-helical, 3–17% β-sheet and 26–44% random coil), however all proteins (with the exception of C335A-IDO) maintained similar proportions of α-helical, β-sheet and random coil structure (*i.e.* % α-helix > % random coil > % β-sheet). In the case of protein C335A-IDO, the percentage of random coil was higher than both α-helix and β-sheet. Interestingly, the residue C335 is in close proximity to the cofactor entrance flexible loop (residues 360–380 – unresolved by X-ray crystallography) of IDO1. The mutation of C335A appears to alter a segment of the large domain (Fig. 1 – Red) resulting in the increased proportion of random coil observed for this enzyme.

Generally, far UV CD spectroscopy indicated that site-directed mutagenesis of individual cysteine residues had only subtle effects on overall protein secondary structure. Spectra were obtained at high protein concentrations, which allowed greater sensitivity of

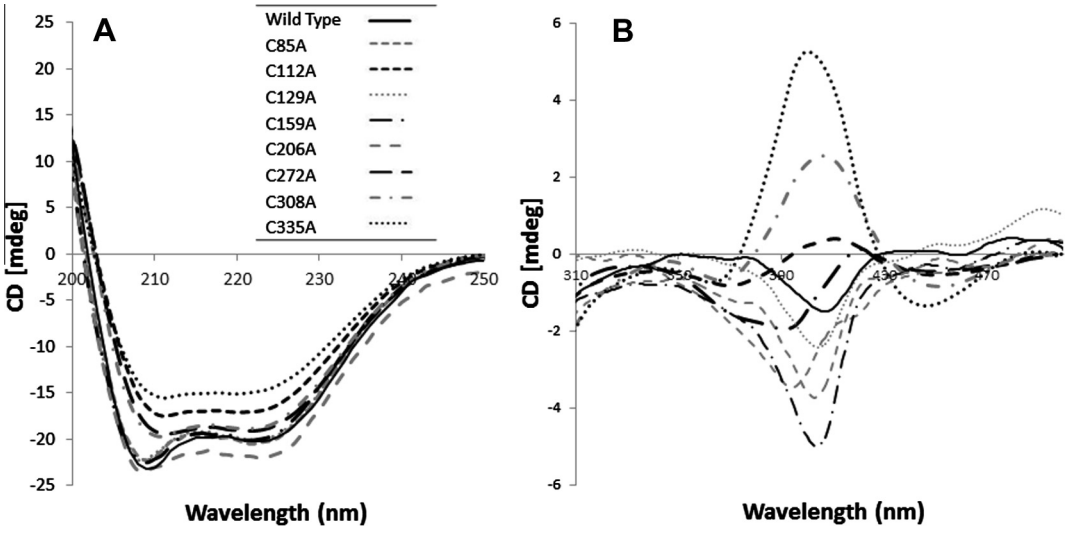

Fig. 2. (A) Circular dichroism spectra of mutant and wild type IDO1 proteins. CD spectra were conducted in 10 mM Tris (pH 7.4) buffer with a 10 mm pathlength cuvette. Protein concentration: 1 mg/mL. The region 200–250 nm is shown. (B) Circular dichroism spectra of mutant and wild type IDO1 proteins. CD spectra were conducted in a 1 mm pathlength cuvette. Protein concentration: 5–10 mg/mL. The region 310–500 nm is shown.

Table 1
Secondary structure analyses of wild type IDO1 and cysteine to alanine IDO1 mutants.

IDO1	α-Helix (%)	β-Sheet (%)	Random coil (%)
Wild Type	62.92	4.24	32.84
C85A	70.48	3.49	26.03
C112A	43.66	14.49	41.85
C129A	70.54	3.43	26.03
C159A	70.68	3.42	25.9
C206A	65.65	3.43	30.92
C272A	49.45	10.93	39.62
C308A	49.72	10.6	39.68
C335A	38.64	17.27	44.09

both the aromatic amino acid side chain and heme environments, respectively. All proteins were oxidised, showing UV–Vis absorbance maxima at 406 nm (Supplementary Data). Overlay of the 310–500 nm CD spectral data reveals measurable changes to mutant IDO1 spectra when compared to wild type, indicating structural changes to the environment of the heme B cofactor (Fig. 2B). For example, C85A-IDO1 shows two distinct peaks at 395 nm and 420 nm – this Soret peak splitting is possibly due to lowered effective symmetry of the heme B group resulting in a lift to the degeneracy of the π^* molecular orbital associated with the Soret transition [17]. Although the present results do not allow us to specify how amino acid substitution affects the heme B moiety (*e.g.* torsion, doming or out of plane twisting due to indirect structural changes), when viewed in conjunction with substrate kinetic data (see *Biochemical Analysis* below), the near UV/Soret spectral changes reveal that only subtle changes are required to alter the normal orientation of critical residues and the heme group within the active site.

The thermal transitions of wild type and mutant IDO1 proteins were monitored by measuring molar ellipticity at $\lambda = 222$ nm (α-helix region) as a function of the increasing temperature over the range 20–99 °C (Fig. 3). T_m values for wild type and mutant proteins were determined from the first derivative of the melting curves (Fig. 3 inset). No protein sample refolded upon cooling. A small global increase in stability was observed in C206A-IDO1 over wild type IDO1, however for all other mutant proteins loss of thermal stability was observed. C206 is located in the large (Fig. 1 – red) IDO1 protein domain and alanine substitution has increased the percentage of α-helix structure within the mutant protein when compared to wild type IDO1 (Table 1). The small increase to highly ordered α-helix may explain the slower rate of denaturation observed in C206A-IDO1.

3.2. Biochemical analysis of wild type and mutant IDO1 species

The enzymatic activity of wild type IDO1 and each mutant-IDO1 protein was analysed using L-tryptophan and D-tryptophan as substrates. The kinetic parameters of wild type and mutant IDO1 for L-tryptophan and D-tryptophan are given in Table 2. For L-tryptophan, all mutants showed a decrease in enzymatic efficiency when compared to the wild type IDO1, with C85A-IDO1 and C206A-IDO1 showing the largest V_{max}/K_m reductions of 86% and 85%, respectively. Interestingly, both these proteins displayed measurable differences in their spectroscopic characteristics (*i.e.* Soret peak splitting and thermal stability changes, respectively) when compared to wild type IDO1, thus providing supporting data to conclude that cysteine mutation has altered both protein structure and function, particularly in relation to the cofactor binding site. Residue C206, for example, is located on the same α-helix as 'gating' residues F226, F227 and R231, which are critical to IDO1 substrate recognition (Fig. 4A). The loss of L-tryptophan enzymatic activity observed for C206A-IDO1 may be due to an alteration of the hydrophobic interactions and stabilisation bonds provided by F226, F227 and R231 to the heme-binding pocket of wild type IDO1 [16], resulting from mutation of C206 to Alanine. Residue C85 (Fig. 1 – small domain, blue) is located at the cleft joining the large and small domains of IDO1. Due to its spatial position (Fig. 4B), C85 is unlikely to interact directly with substrate, however, the substitution of the bulky aromatic cysteine residue with the simple, smaller alanine residue may change contact/binding between domains by altering hydrophobic interactions, salt

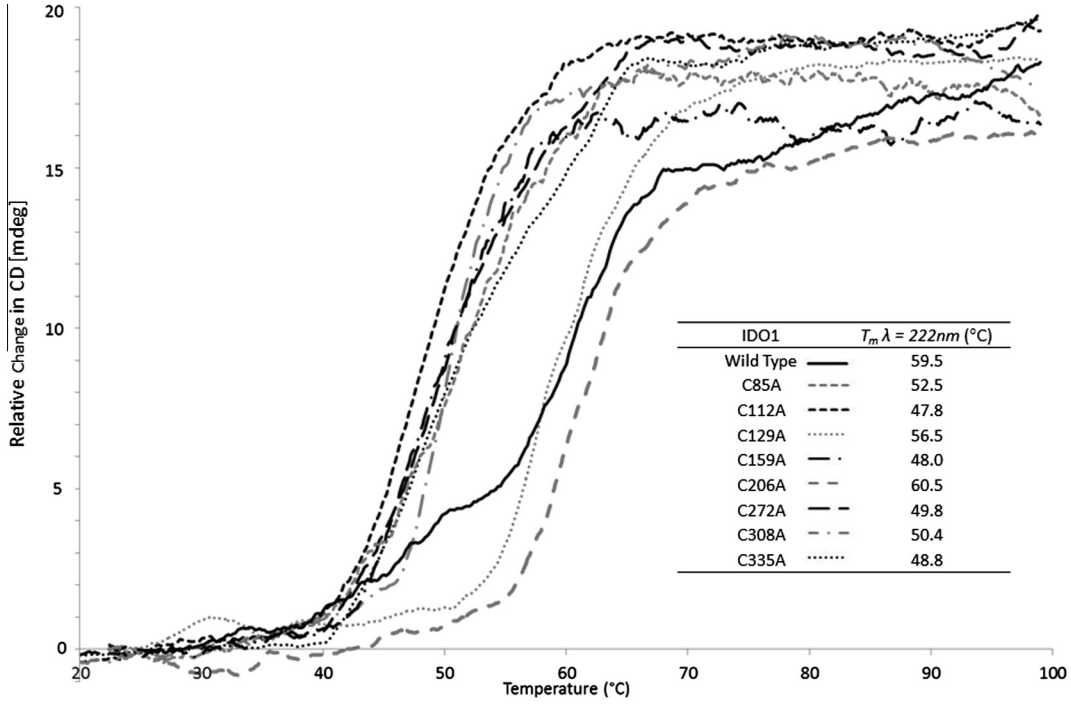

Fig. 3. Thermal transition of mutant and wild type IDO1 proteins at $\lambda = 222$ nm over the range 20–99 °C.

Table 2
Kinetic parameters of wild type and mutant IDO1 for L-tryptophan and D-tryptophan.

IDO1	L-tryptophan			D-tryptophan		
	V_{max} min^{-1}	K_m μM	V_{max}/K_m μM^{-1} min^{-1}	V_{max} min^{-1}	K_m mM	V_{max}/K_m mM^{-1} min^{-1}
Wild type	120	20	**6**	160	5	**32**
C85A	30.6 ± 2.0	35.9	**0.852**	85.3 ± 3.8	2.1	**41**
C112A	59.8 ± 1.5	18.7 ± 2.0	**3.2**	109.4 ± 0.6	1.3 ± 0.0	**85**
C129A	101.1 ± 15.0	42.3	**2.39**	31.4 ± 1.3	3.7	**8.5**
C159A	110.4 ± 2.5	75.9	**1.45**	40.3 ± 3.5	4.4	**9.2**
C206A	45.5 ± 2.6	50.9	**0.894**	64.7 ± 3.4	1.7	**38**
C272A	51.2 ± 0.4	38.1 ± 0.9	**1.3**	101.0 ± 1.3	3.7 ± 0.2	**28**
C308A	94.3 ± 2.4	90.3 ± 5.3	**1.0**	117.5 ± 1.7	3.3 ± 0.2	**35**
C335A	56.8 ± 0.6	17.1 ± 0.8	**3.3**	96.1 ± 4.2	9.5 ± 0.9	**10.1**

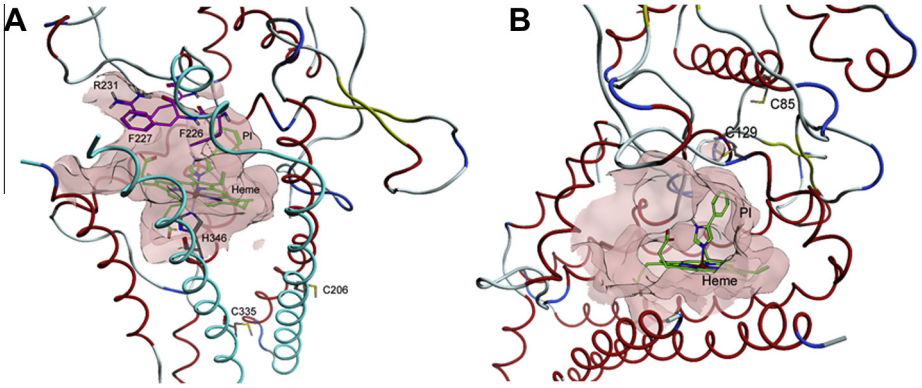

Fig. 4. (A) Crystal structure of wild type IDO-1 showing C206 and C335 relative to the active site (PDB: 2D0T). Carbon atoms of co-crystalised phenylimidazole (PI) and heme are coloured green. Carbon atoms of gating residues F226, F227 and R231 are coloured fuschia. C206 is directly connected to the gating residues *via* a rigid alpha helix (colour cyan for contrast). C335 is directly connected to the heme-binding residue H346 (grey carbons, helix also in cyan). With both helices running parallel, structural changes are potentially transmitted to the heme and/or the gating residues *via* these rigid structures. (B) Crystal structure of wild type rhIDO-1 showing the proximity between C85 and C129 (5.7 angstroms) and the heme active site (PDB: 2D0T, [16]). C129 makes up the roof of the indole binding pocket (occupied here by the phenyl ring of co-crystalised phenylimidazole, PI). (For interpretation of the references to colour in this figure legend, the reader is referred to the web version of this article.)

bridges, or hydrogen bonding resulting in the observed loss of metabolic activity. Any changes to the active site of C85A-IDO1 is likely mediated through C129 (Fig. 4B), which is positioned in-between the heme group and C85, and forms part of the roof of the IDO1 active site.

A large drop (69%) in D-tryptophan metabolism was observed in C335A-IDO1 (Table 2; Fig. 4A). Given the substantial alteration in secondary structure observed for the mutant enzyme C335A-IDO1 (increased proportion of random coil – see *Structural Analysis*), its location on the same long α-helix chain as the proximal co-ordination binding residue (Histidine 346) and proximity to the flexible loop of IDO1 located at the entrance to the cofactor active site, a significant change in substrate efficiency is not unexpected. Interestingly, proteins C85A-IDO1, C112A-IDO1 and C206A-IDO1 showed an increased ability to convert D-tryptophan when measured against the efficiency of the wild-type, with C112A-IDO1 showing the highest increase (265%). This would indicate that while amino acid modification has affected the ability of L-tryptophan to interact with the heme b co-factor, protein structure modification has altered D-tryptophan substrate accessibility. From these results, it is clear that cysteine residues play a role in maintaining the strict geometric complementarity that is required for the formation of the substrate/co-factor complex and the normal enzymatic function of wild type IDO1.

This study is the first to investigate the role cysteine residues play in the metabolic stability of IDO1. While not involved directly in heme b binding or disulphide bond formation, cysteine residues within IDO1 play an important role in the maintenance and stability of normal structure and kinetic behaviour.

Appendix A. Supplementary data

Supplementary data associated with this article can be found, in the online version, at http://dx.doi.org/10.1016/j.bbrc.2013.05.119.

References

[1] H.J. Yuasa, H.J. Ball, Y.F. Ho, C.J. Austin, C.M. Whittington, K. Belov, G.J. Maghzal, L.S. Jermiin, N.H. Hunt, Characterization and evolution of vertebrate indoleamine 2, 3-dioxygenases IDOs from monotremes and marsupials, Comp. Biochem. Physiol. B Biochem. Mol. Biol. 153 (2009) 137–144.
[2] M. Friberg, R. Jennings, M. Alsarraj, S. Dessureault, A. Cantor, M. Extermann, A.L. Mellor, D.H. Munn, S.J. Antonia, Indoleamine 2,3-dioxygenase contributes to tumor cell evasion of T cell-mediated rejection, Int. J. Cancer 101 (2002) 151–155.
[3] E.A. Bonney, P. Matzinger, Much IDO about pregnancy, Nat. Med. 4 (1998) 1128–1129.
[4] D.H. Munn, M. Zhou, J.T. Attwood, I. Bondarev, S.J. Conway, B. Marshall, C. Brown, A.L. Mellor, Prevention of allogeneic fetal rejection by tryptophan catabolism, Science 281 (1998) 1191–1193.
[5] G.J. Guillemin, G. Smythe, O. Takikawa, B.J. Brew, Expression of indoleamine 2,3-dioxygenase and production of quinolinic acid by human microglia, astrocytes, and neurons, Glia 49 (2005) 15–23.
[6] N.H. Hunt, J. Golenser, T. Chan-Ling, S. Parekh, C. Rae, S. Potter, I.M. Medana, J. Miu, H.J. Ball, Immunopathogenesis of cerebral malaria, Int. J. Parasitol. 36 (2006) 569–582.
[7] A. Okamoto, T. Nikaido, K. Ochiai, S. Takakura, M. Saito, Y. Aoki, N. Ishii, N. Yanaihara, K. Yamada, O. Takikawa, R. Kawaguchi, S. Isonishi, T. Tanaka, M. Urashima, Indoleamine 2,3-dioxygenase serves as a marker of poor prognosis in gene expression profiles of serous ovarian cancer cells, Clin. Cancer Res. 11 (2005) 6030–6039.
[8] M. Arefayene, S. Philips, D. Cao, S. Mamidipalli, Z. Desta, D.A. Flockhart, D.S. Wilkes, T.C. Skaar, Identification of genetic variants in the human indoleamine 2, 3-dioxygenase (IDO1) gene, which have altered enzyme activity, Pharmacogenet. Genom. 19 (2009) 464–476.

[9] C.J. Austin, J. Mizdrak, A. Matin, N. Sirijovski, P. Kosim-Satyaputra, R.D. Willows, T.H. Roberts, R.J. Truscott, G. Polekhina, M.W. Parker, J.F. Jamie, Optimised expression and purification of recombinant human indoleamine 2,3-dioxygenase, Protein Exp. Purif. 37 (2004) 392–398.
[10] U.K. Laemmli, Cleavage of structural proteins during the assembly of the head of bacteriophage T4, Nature 227 (1970) 680–685.
[11] C.J. Austin, F. Astelbauer, P. Kosim-Satyaputra, H.J. Ball, R.D. Willows, J.F. Jamie, N.H. Hunt, Mouse and human indoleamine 2,3-dioxygenase display some distinct biochemical and structural properties, Amino Acids 36 (2009) 99–106.
[12] C.J. Austin, B.M. Mailu, G.J. Maghzal, A. Sanchez-Perez, S. Rahlfs, K. Zocher, H.J. Yuasa, J.W. Arthur, K. Becker, R. Stocker, N.H. Hunt, H.J. Ball, Biochemical characteristics and inhibitor selectivity of mouse indoleamine 2,3-dioxygenase-2, Amino Acids 39 (2010) 565–578.
[13] O. Takikawa, T. Kuroiwa, F. Yamazaki, R. Kido, Mechanism of Interferon-γ action; Characterisation of indoleamine 2,3-dioxygenase in cultured human cells induced by interferon-γ and evaluations of the enzyme-mediated tryptophan degradation in its anticellular activity, J. Biol. Chem. 263 (1988) 2041–2048.
[14] T.K. Littlejohn, O. Takikawa, R.J. Truscott, M.J. Walker, Asp274 and his346 are essential for heme binding and catalytic function of human indoleamine 2,3-dioxygenase, J. Biol. Chem. 278 (2003) 29525–29531.
[15] T. Shimizu, S. Nomiyama, F. Hirata, O. Hayaishi, Indoleamine 2,3-dioxygenase, purification and some propertities, J. Biol. Chem. 253 (1978) 4700–4706.
[16] H. Sugimoto, S. Oda, T. Otsuki, T. Hino, T. Yoshida, Y. Shiro, Crystal structure of human indoleamine 2,3-dioxygenase: catalytic mechanism of O_2 incorporation by a heme-containing dioxygenase, Proc. Natl. Acad. Sci. USA 103 (2006) 2611–2616.
[17] J.S. Felsch, M.P. Horvath, S. Gursky, M.R. Hobaugh, P.N. Goudreau, J.A. Fee, W.T. Morgan, S.J. Admiraal, M. Ikeda-Saito, T. Fujiwara, et al., Probing protein-cofactor interactions in the terminal oxidases by second derivative spectroscopy: study of bacterial enzymes with cofactor substitutions and heme a model compounds, Protein Sci. 3 (1994) 2097–2103.